Hydrogen Production Hot Paper

Deutsche Ausgabe: DOI: 10.1002/ange.201603528
Internationale Ausgabe: DOI: 10.1002/anie.201603528

A Highly Efficient Sandwich-Like Symmetrical Dual-Phase Oxygen-Transporting Membrane Reactor for Hydrogen Production by Water Splitting

Wei Fang, Frank Steinbach, Zhongwei Cao, Xuefeng Zhu,* and Armin Feldhoff**

Abstract: *Water splitting coupled with partial oxidation of methane (POM) using an oxygen-transporting membrane (OTM) would be a potentially ideal way to produce high-purity hydrogen as well as syngas. Over the past decades, substantial efforts have been devoted to the development of supported membranes with appropriate configurations to achieve considerable performance improvements. Herein, we describe the design of a novel symmetrical membrane reactor with a sandwich-like structure, whereby a largescale production ($>10\,mL\,min^{-1}\,cm^{-2}$) of hydrogen and syngas can be obtained simultaneously on opposite sides of the OTM. Furthermore, this special membrane reactor could regenerate the coke-deactivated catalyst in situ by water steam in a single unit. These results represent an important first step in the development of membrane separation technologies for the integration of multiple chemical processes.*

Hydrogen, as a clean energy carrier, can play a key role in major industrial processes.[1] Generally, the world's hydrogen supply comes from the reformation of fossil fuels, which increases the concentration of atmospheric CO_2.[2] Thus, the generation of hydrogen through water splitting is becoming an especially attractive alternative because water is considered as the ideal source owing to its abundance.[3] However, efficient hydrogen production from water is quite difficult as a result of the very low equilibrium constant ($K_p \approx 2.1 \times 10^{-8}$) even at a relatively high temperature of 900 °C.[4] Relatively recently, an oxygen-transporting membrane (OTM) reactor, consisting of mixed ionic and electronic conducting (MIEC) materials, was applied to the water splitting reaction.[5] On the feed side of the OTM, water was dissociated into hydrogen and oxygen species. Afterwards, oxygen species were transported as oxygen ions through the OTM. To ensure rapid removal of oxygen, methane/biomethane was fed on the sweep side of the membrane to consume the permeated oxygen by partial oxidation of methane (POM) to syngas. Consequently, a higher production rate of hydrogen was obtained. However, cheap Ni-based catalysts are prone to deactivation as a result of coke deposition (that is, carbon buildup) once pure methane has been used as the feedstock, similar to the effect observed in industrial processes for methane reforming.[6] Although great efforts have been focused on the development of coke-resistant catalysts,[7] coke-deposition-induced performance degradation is still difficult to avoid. To maximize the function of the OTM, it is crucial to balance the high chemical stability and the practical oxygen permeability. When cobalt/copper-containing perovskite oxides (for example, $Ba_{0.5}Sr_{0.5}Co_{0.8}Fe_{0.2}O_{3-\delta}$) are employed as membrane materials, the performance of the reactor may gradually degrade with time because of the easily reducible active cations.[8] As compared to perovskites, fluorite-type ceria-based oxides exhibit fast oxygen-ion mobility and good redox catalytic properties.[9] Unfortunately, the electronic conductivities of such ionic conducting (IC) ceria derivatives are found to be the major bottleneck for oxygen permeation.[10] Thus, an MIEC–IC composite dual-phase membrane is believed to be a prospective candidate for application in chemical reactors (Figure 1).[11]

To date, tremendous efforts have been made to improve the oxygen permeability by designing supported/thin membranes and modifying their surfaces.[12] Herein, we present a dual-phase OTM reactor with a sandwich-like symmetrical configuration, whereby two porous backbones built up on both side of the dense functional layer may alleviate the

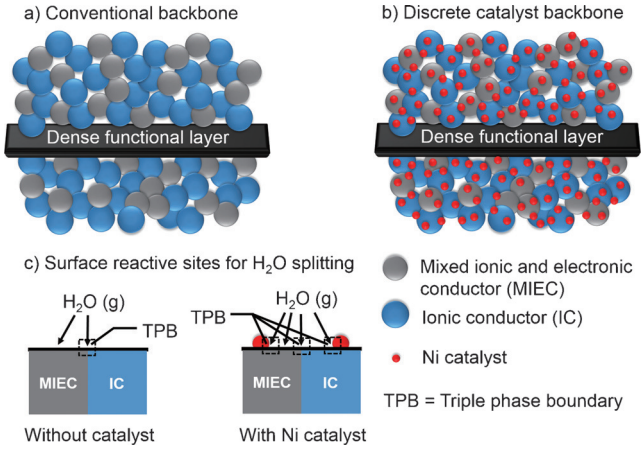

Figure 1. Schematic diagrams of a) the conventional blank backbone with a random mixture of an MIEC and an IC material; b) the Ni-catalyst-impregnated MIEC/IC composite backbone; and c) activity enhancement of the Ni-infiltrated backbone for H_2O splitting.

[*] W. Fang, F. Steinbach, Prof. Dr. A. Feldhoff
Institute of Physical Chemistry and Electrochemistry
Leibniz University Hannover
Callinstrasse 3A, 30167 Hannover (Germany)
E-mail: wei.fang@pci.uni-hannover.de
armin.feldhoff@pci.uni-hannover.de

Z. W. Cao, Prof. Dr. X. F. Zhu
State Key Laboratory of Catalysis
Dalian Institute of Chemical Physics
Chinese Academy of Sciences
457 Zhongshan Road, Dalian 116023 (China)
E-mail: zhuxf@dicp.ac.cn

Supporting information for this article can be found under: http://dx.doi.org/10.1002/anie.201603528.

performance losses caused by slow surface-reaction kinetics (Figure 1 a).[13] Additionally, the thinner dense layer obviously decreases the bulk diffusion resistance for the oxygen ionic transport.[13] Remarkably, the amounts of possible reaction sites can be further increased by chemical infiltration processes.[14] The backbones were impregnated with a Ni catalyst to increase the number of triple phase boundary (TPB) sites[15] for water splitting reactions (Figure 1 b,c), as well as to catalyze the POM reaction. We also foresaw that coking could probably accompany the syngas production,[6,7] which deactivates the catalyst and leads to a decrease of the hydrogen production rate from water. In this work, we propose that water (steam) can be used not only as a hydrogen source, but also as a "coke cleaner" to regenerate in situ the Ni catalyst in a sandwich-like symmetrical reactor by simply switching valves without stopping the reactions. As a result, three separate chemical reactions (water splitting, partial oxidation of methane, and carbon removal by steam) are integrated in one unit, which may contribute to the intensification of industrial processes.[16]

A recently developed dual-phase OTM based on $Ce_{0.85}Sm_{0.15}O_{1.925}$ (75 wt.%)/$Sm_{0.6}Sr_{0.4}Al_{0.3}Fe_{0.7}O_{3-\delta}$ (25 wt.%), denoted SDC–SSAF, shows particularly promising and stable oxygen permeability under reducing conditions (see Figure S1 in the Supporting Information).[17] Therefore, a novel SDC–SSAF sandwich-like symmetrical membrane was applied to the water splitting reaction. The cross-sectional morphologies of the sintered SDC–SSAF membrane with Ni infiltration are shown in Figure 2. It can be clearly seen that the sandwich-like symmetrical membrane comprises one thin dense layer with a thickness of about 30 μm and two thick porous backbones, each with a thickness of about 500 μm (Figure 2 a–c). To better understand the nature of the Ni catalyst and its role in the reaction process, a magnified secondary electron (SE) micrograph was collected, which demonstrates that the Ni nanoparticles (diameter: approximately 100–700 nm) have tightly covered the surface of the backbone and are randomly distributed (Figure 2 d). Furthermore, the elemental distribution was identified by energy-dispersive X-ray spectroscopy (EDXS; Figure S2).

First, the oxygen permeability and stability of the non-infiltrated SDC–SSAF membrane was investigated. Figure 3 displays the long-term oxygen permeation of the membrane under three operational conditions. When helium was used as the sweep gas (with air as the feed gas), the permeation fluxes

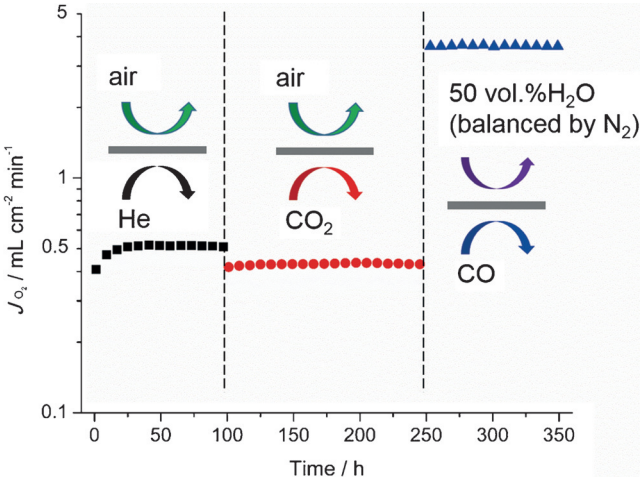

Figure 3. Long-term oxygen permeation rates (J_{O_2}) through the non-infiltrated SDC–SSAF symmetrical dual-phase membrane. Conditions: air = 100 mL min^{-1} or H_2O = 50 mL min^{-1} (balanced by 50 mL min^{-1} N_2) as the feed gas; He = 50 mL min^{-1} or CO_2 = 30 mL min^{-1} or CO = 30 mL min^{-1} as the sweep gas, respectively. 1 mL min^{-1} Ne as the internal standard gas. Temperature = 950 °C.

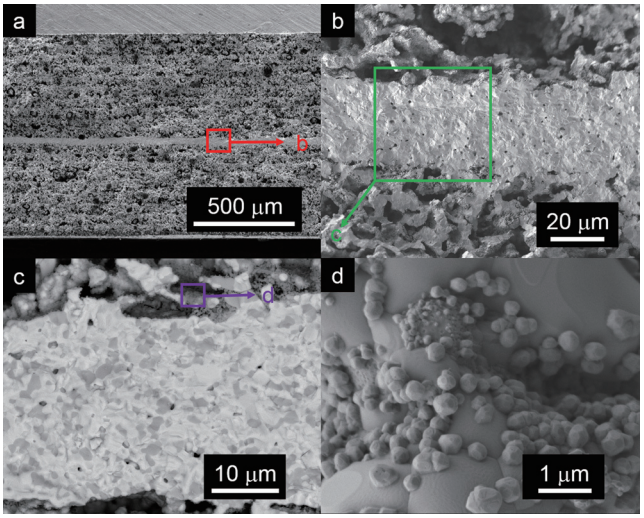

Figure 2. Cross-sectional microstructure of the Ni-infiltrated SDC–SSAF sandwich-like symmetrical dual-phase OTM. Secondary electron (SE) micrographs showing a) an overview and b) an expanded portion of the dense functional layer. c) Backscattered electron (BSE) micrograph of the dense layer. The light grains are the SDC phase, and the dark grains are the SSAF phase. d) Magnified SE micrograph of the impregnated Ni catalyst.

increased quickly with time for the initial 25 h, and then reached a relatively steady state. This phenomenon was also observed with other dual-phase membranes, and can be ascribed to the readjusting or reoxidation of the lattice structure from the as-prepared to the operational state.[18] Subsequently, CO_2 was selected as reactive sweep gas. In this operation, a small decrease in the oxygen permeation rate (J_{O_2}) from 0.51 to 0.42 mL min^{-1} cm^{-2} was initially observed as a result of the decrease in the oxygen surface exchange rate resulting from CO_2 adsorption.[19] However, no further degradation of oxygen flux was detected after 150 h of operation, indicating that the membrane is sufficiently tolerant towards CO_2.

Finally, water splitting was conducted in the membrane reactor. Since hydrogen generation from water depends strongly on the oxygen permeability of the membrane, a larger driving force for oxygen transport can bring about a higher hydrogen production rate. Accordingly, a reducing gas (carbon monoxide) was employed as the sweep gas (with water steam as the feed gas). These changes led to a sevenfold increase in the oxygen permeation rate compared to that obtained with helium as the sweep gas (and air as the feed gas). Additionally, the membrane reactor

maintained a stable performance over 100 h of operation, which indicates good chemical stability under conditions suitable for water splitting. However, the oxidation of CO renders the method less useful. Therefore, it would be more attractive to combine the partial oxidation of methane (POM) to produce syngas (primarily for Fischer–Tropsch synthesis)[20] in the reactor.

Along with the above-mentioned experiments, the production of hydrogen by water splitting coupled with POM was carried out in a Ni-infiltrated SDC–SSAF membrane reactor (Figure 4). As expected, a very high hydrogen production rate

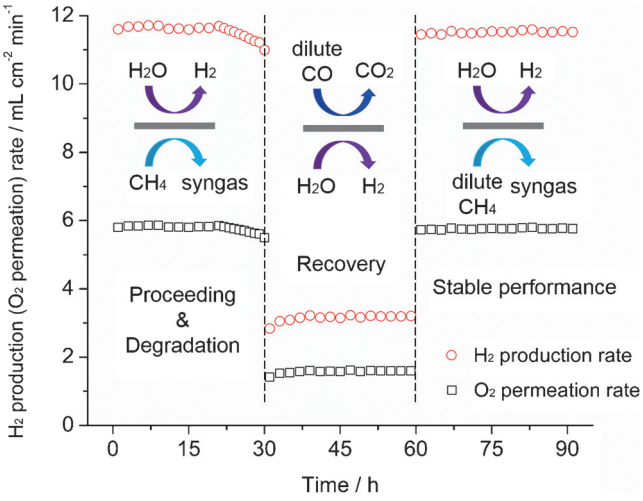

Figure 4. H_2 production and O_2 permeation rates as a function of time through the Ni-infiltrated SDC–SSAF symmetrical dual-phase membrane. Flow rate conditions: $H_2O = 50\ mL\,min^{-1}$ (balanced by $50\ mL\,min^{-1}\ N_2$); pure $CH_4 = 5.84\ mL\,min^{-1}$; dilute $CO = 3\ mL\,min^{-1}$ $CO + 20\ mL\,min^{-1}$ He; dilute $CH_4 = 5\ mL\,min^{-1}$ $CH_4 + 5\ mL\,min^{-1}$ He. $Ne = 1\ mL\,min^{-1}$ was used as the internal standard gas. Temperature = 900 °C.

of $11.7\ mL\,min^{-1}\,cm^{-2}$ was firstly achieved as a result of the increased oxygen permeability ascribed to fast surface exchange kinetics[13] through Ni infiltration. It is worth noting that the hydrogen production rate declined after 20 h of operation, rapidly decreasing by 6% of its starting value within 10 h. It is likely that this deterioration can be attributed to undesirable coking of the catalyst. According to current knowledge in the field of Ni-based catalysts, water is considered to be the most effective inhibitor of carbon buildup.[21] In an attempt to recover the performance of the membrane reactor, the water splitting reaction was conducted on the previous sweep side to simultaneously regenerate the catalyst in situ (dilute CO was used on the other side). The oxygen (hydrogen) fluxes were found to gradually increase over the next 8 h, then reaching a plateau. To make sure that coke has been successfully removed, dilute methane was applied to the sweep side afterwards. Generally, it is thought that lowering the concentration of methane decreases the oxygen permeation (hydrogen production) rate because of a smaller oxygen partial pressure gradient across the OTM.[13] However, the dilute methane with a higher flow rate can overcome the diffusion resistance of the porous backbone (Figure S5), resulting in a higher methane conversion rate compared with pure methane in principle. Note that a slightly lower but stable hydrogen (oxygen) flux was subsequently obtained during 30 h of operation for helium-diluted methane. This means that to some degree, coking can be avoided when dilute methane is used. A more reasonable explanation is that the ratio of O_2:CH_4 has a significant influence on coking,[22] that is, a higher O_2:CH_4 ratio leads to a higher resistance to coking (coking occurs easily at a ratio of O_2:$CH_4 \approx 1{:}2$ for pure methane, but hardly at O_2:$CH_4 > 1{:}2$ for helium-diluted methane).

Figure 5 shows the selectivity of CO_2 (or CO) and the conversion of methane with time in the membrane reactor (which also supports the above conclusion). Compared with the relatively stable values obtained under an atmosphere of dilute methane, the selectivity of CO_2 declined from 5.18% to

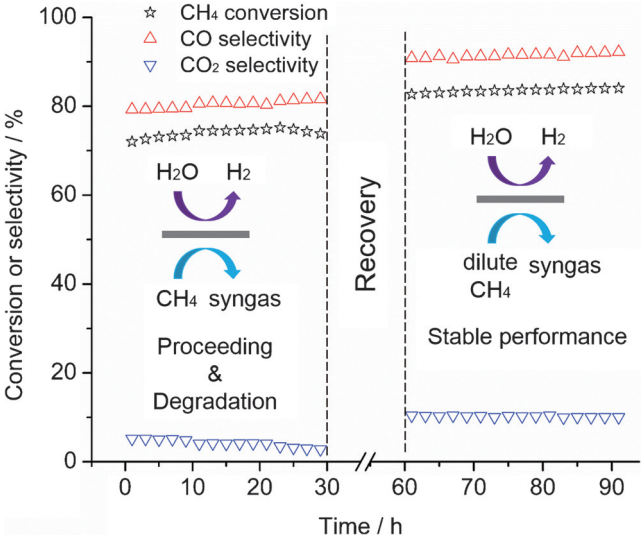

Figure 5. Conversion of methane and selectivity of CO or CO_2 as a function of time in the Ni-infiltrated SDC–SSAF symmetrical dual-phase membrane reactor. Flow rate conditions: $H_2O = 50\ mL\,min^{-1}$ (balanced by $50\ mL\,min^{-1}\ N_2$); pure $CH_4 = 5.84\ mL\,min^{-1}$; dilute $CH_4 = 5\ mL\,min^{-1}$ $CH_4 + 5\ mL\,min^{-1}$ He. $Ne = 1\ mL\,min^{-1}$ was used as the internal standard gas. Temperature = 900 °C.

2.82% within 30 h in the presence of pure methane. This result demonstrates that the partial oxidation of methane is more favorable than the total oxidation of methane. Moreover, the selectivity value of CO_x (the sum of CO_2 and CO) was far from 100% in pure methane, but was very close to 100% for the dilute case. This clearly suggests that coking occurred in the reactor when using pure methane as the sweep gas (Figure S3), as also indicated by the fact that the line denoting methane conversion became curved with time (another indication of catalyst deactivation). However, helium-diluted methane was used as part of a proof-of-principle study limited for laboratory use, as for widespread application in industry pure methane is used. Fortunately, the catalyst can be completely regenerated in our symmetrical membrane system, enabling the sustaining production of hydrogen from water.

In conclusion, this work presents an approach to obtain considerably high hydrogen production rates (Table S1) through water splitting coupled with POM by means of a dual-phase OTM with a sandwich-like symmetrical structure. However, the performance of the membrane reactor may degrade as a result of catalyst deactivation (coking). It is demonstrated first that the catalyst can be regenerated in situ in a single unit by conducting the water splitting reaction on the catalyst-deactivated side. This discovery will enable us to gain new insight into the interplay between catalysis (recovery) and separation in the OTM reactor, and accelerate the pace of development of next-generation practical OTM applications.

Acknowledgements

This work has been supported by the German Research Foundation (DFG; no. FE928/7-1) and the Natural Science Foundation of China (21271169 and 21476225). We also acknowledge A. Wollbrink and W. Y. Liang for technical support.

Keywords: catalyst regeneration · hydrogen production · membrane reactor · methane · water splitting

How to cite: *Angew. Chem. Int. Ed.* **2016**, *55*, 8648–8651
Angew. Chem. **2016**, *128*, 8790–8793

[1] M. D. Symes, L. Cronin, *Nat. Chem.* **2013**, *5*, 403–409.
[2] S. J. Davis, K. Caldeira, H. D. Matthews, *Science* **2010**, *329*, 1330–1333.
[3] J. A. Turner, *Science* **2004**, *305*, 972–974.
[4] S. Ihara, *Bull. Electrotech. Lab.* **1977**, *41*, 259–280.
[5] a) H. Q. Jiang, H. H. Wang, S. Werth, T. Schiestel, J. Caro, *Angew. Chem. Int. Ed.* **2008**, *47*, 9341–9344; *Angew. Chem.* **2008**, *120*, 9481–9484; b) U. Balachandran, T. H. Lee, S. E. Dorris, *Int. J. Hydrogen Energy* **2007**, *32*, 451–456.
[6] a) D. L. Trimm, *Catal. Today* **1999**, *49*, 3–10; b) Y. B. Lin, Z. L. Zhan, J. Liu, S. A. Barnett, *Solid State Ionics* **2005**, *176*, 1827–1835.
[7] a) D. Neagu, T. S. Oh, D. N. Miller, H. Ménard, S. M. Bukhari, S. R. Gamble, R. J. Gorte, J. M. Vohs, J. T. S. Irvine, *Nat. Commun.* **2015**, *6*, 8120; b) Y. Chen, Y. X. Zhang, Y. Lin, Z. B. Yang, D. Su, M. F. Han, F. L. Chen, *Nano Energy* **2014**, *10*, 1–9.
[8] a) Z. P. Shao, H. Dong, G. X. Xiong, Y. Cong, W. S. Yang, *J. Membr. Sci.* **2001**, *183*, 181–192; b) M. Harada, K. Domen, M. Hara, T. Tatsumi, *Chem. Lett.* **2006**, *35*, 968–969; c) W. Q. Jin, S. G. Li, P. Huang, N. P. Xu, J. Shi, Y. S. Lin, *J. Membr. Sci.* **2000**, *166*, 13–22.
[9] M. Mogensen, N. M. Sammes, G. A. Tompsett, *Solid State Ionics* **2000**, *129*, 63–94.
[10] M. Balaguer, C. Solís, J. M. Serra, *Chem. Mater.* **2011**, *23*, 2333–2343.
[11] a) V. V. Kharton, A. V. Kovalevsky, A. P. Viskup, A. L. Shaula, F. M. Figueiredo, E. N. Naumovich, F. M. B. Marques, *Solid State Ionics* **2003**, *160*, 247–258; b) X. F. Zhu, Q. M. Li, Y. F. He, Y. Cong, W. S. Yang, *J. Membr. Sci.* **2010**, *360*, 454–460; c) S. Y. Cheng, H. Huang, S. Ovtar, S. B. Simonsen, M. Chen, W. Zhang, M. Søgaard, A. Kaiser, P. V. Hendriksen, C. S. Chen, *ACS Appl. Mater. Interfaces* **2016**, *8*, 4548–4560; d) W. Fang, F. Y. Liang, Z. W. Cao, F. Steinbach, A. Feldhoff, *Angew. Chem. Int. Ed.* **2015**, *54*, 4847–4850; *Angew. Chem.* **2015**, *127*, 4929–4932; e) Z. B. Zhang, W. Zhou, Y. B. Chen, D. J. Chen, J. W. Chen, S. M. Liu, W. Q. Jin, Z. P. Shao, *ACS Appl. Mater. Interfaces* **2015**, *7*, 22918–22926.
[12] a) K. Watenabe, M. Yuasa, T. Kida, Y. Teraoka, N. Yamazoe, K. Shimanoe, *Adv. Mater.* **2010**, *22*, 2367–2370; b) X. Y. Tan, Y. T. Liu, K. Li, *AIChE J.* **2005**, *51*, 1991–2000; c) Y. Y. Wei, H. F. Liu, J. Xue, Z. Li, H. H. Wang, *AIChE J.* **2011**, *57*, 975–984; d) J. H. Joo, K. S. Yun, Y. Lee, J. Jung, C. Y. Yoo, J. H. Yu, *Chem. Mater.* **2014**, *26*, 4387–4394; e) S. Liu, X. Tan, Z. Shao, J. C. Diniz da Costa, *AIChE J.* **2006**, *52*, 3452–3461; f) S. Baumann, J. M. Serra, M. P. Lobera, S. Escolástico, F. Schulze-Küppers, W. A. Meulenberg, *J. Membr. Sci.* **2011**, *377*, 198–205; g) J. W. Zhu, Z. Y. Dong, Z. K. Liu, K. Zhang, G. R. Zhang, W. Q. Jin, *AIChE J.* **2014**, *60*, 1969–1976.
[13] *Fundamentals of Inorganic Membrane Science and Technology* (Eds.: H. J. M. Bouwmeester, A. J. Burggraaf, L. Cot), Elsevier, Amsterdam, **1996**, pp. 435–528.
[14] a) J. M. Vohs, R. J. Gorte, *Adv. Mater.* **2009**, *21*, 943–956; b) D. Ding, M. F. Liu, Z. B. Liu, X. X. Li, K. Blinn, X. B. Zhu, M. L. Liu, *Adv. Energy Mater.* **2013**, *3*, 1149–1154; c) S. Kim, A. Jun, O. Kwon, J. Kim, S. Yoo, H. Y. Jeong, J. Shin, G. Kim, *ChemSusChem* **2015**, *8*, 3153–3158.
[15] S. B. Adler, *Chem. Rev.* **2004**, *104*, 4791–4843.
[16] K. K. Sirkar, A. G. Fane, R. Wang, S. R. Wickramasinghe, *Chem. Eng. Process.* **2015**, *87*, 16–25.
[17] X. F. Zhu, Y. Liu, Y. Cong, W. S. Yang, *Solid State Ionics* **2013**, *253*, 57–63.
[18] a) X. F. Zhu, W. S. Yang, *AIChE J.* **2008**, *54*, 665–672; b) J. Xue, A. Feldhoff, DOI: 10.1016/j.jeurceramsoc.2016.05.023.
[19] W. Fang, F. Steinbach, C. S. Chen, A. Feldhoff, *Chem. Mater.* **2015**, *27*, 7820–7826.
[20] H. Schulz, *Appl. Catal. A* **1999**, *186*, 3–12.
[21] L. Yang, Y. M. Choi, W. T. Qin, H. Y. Chen, K. Blinn, M. F. Liu, P. Liu, J. M. Bai, T. A. Tyson, M. L. Liu, *Nat. Commun.* **2011**, *2*, 357.
[22] Z. L. Zhan, Y. B. Lin, M. Pillai, I. Kim, S. A. Barnett, *J. Power Sources* **2006**, *161*, 460–465.

Received: April 11, 2016
Published online: May 31, 2016

